JOURNAL OF CATALYSIS 126, 477–488 (1990)

Characteristics of Laboratory-Coked Resid HDS Catalyst

JERRY BAUMGART, YANTI WANG, AND WILLIAM R. ERNST

School of Chemical Engineering, Georgia Institute of Technology, Atlanta, Georgia 30332-0100

AND

J. DONALD CARRUTHERS

Chemical Research Division, American Cyanamid Corporation, 1937 W. Main St., Stamford, Connecticut 06904-00610

Received October 31, 1989; revised July 17, 1990

A sample of commercial residual oil hydrotreating catalyst with a bimodal pore structure was coked to progressively higher levels with styrene at 425°C. Measurements of porosity by mercury intrusion–extrusion porosimetry, nitrogen adsorption–desorption porosimetry, and coronene diffusivity reveal the importance of the pore network to the structure of the coked catalyst. The role played by 'shielded' large pores within the structure is demonstrated. It is proposed that coking first occurs at the junctions between large, shielded pores and narrow connecting pores. The results are discussed in terms of the theoretical predictions of Mann and co-workers. © 1990 Academic Press, Inc.

INTRODUCTION

The relative abundance of heavy crude oil in the world has caused a shift in refining operations from simple 'topping' or distillation processes to 'conversion' processes such as fluid catalytic cracking, coking, and catalytic hydroconversion, where some heavy oil is converted to lighter products. In many cases, conversion processes are preceded by a hydrotreating step in which sulfur, nitrogen, and (for reduced crude residual oils) contaminant metals, nickel and vanadium, are removed from the feed stream. In H-Oil and LC-Fining processes, all of these reactions, including conversion, occur simultaneously.

Hydrotreating catalysts become deactivated when processing residual oils (resids) due to coke deposition and contaminant metals accumulation. Several stages of deactivation have been identified (*1–4*):

1. Rapid coke formation with loss of catalyst activity;
2. Gradual metals deposition on the catalyst, mainly of nickel and vanadium;
3. Rapid catalyst deactivation due to pore mouth plugging with metals.

Deactivation may occur through increased diffusional resistance of reacting molecules in these heavy feeds or through poisoning of the active sites on the catalyst surface.

Both coke deposition and metals accumulation contribute to diffusional resistance but it is the effect of deposited metals at the pore entrances which most often dictates the useful lifespan of the catalyst (pore-mouth plugging). The porous structure of the catalyst is therefore a key factor in the design of catalysts for such service.

Many studies have been reported which describe the influence of metals deposition on the activity and porosity of resid hydrotreating catalysts (*5–7*). Often, spent (deactivated) resid catalysts with contaminant metals and coke were examined. Numerous papers have also been written on catalyst deactivation through coke deposition. How-

0021-9517/90 $3.00

ever, there is still some disagreement about the effect of coke on the catalyst pore structure.

Levinter *et al.* (*8*) studied the kinetics of coke formation of styrene and other hydrocarbons in pelleted silica–alumina cracking catalysts. They found that hydrocarbon structure, catalyst macrostructure, degree of dilution of the hydrocarbon, coking temperature, and other coking conditions influence the coking rate and depth of penetration of coke within the catalyst pellets. Their work provides guidance in selecting coking conditions for laboratory studies.

This report focuses on the influence of coke alone and investigates the changes in porosity of a resid hydrotreating catalyst following stepwise coke deposition. The coking process selected involved the vapor phase decomposition of styrene. We selected styrene for this work because it has a tendency to rapidly form coke deposits within the catalyst under investigation; however, we were able to control the coking rate by highly diluting the styrene with helium and using a coking temperature of 425°C, which is at the low end of the temperature range studied by Levinter *et al.* (*8*). All catalyst samples were coked after crushing in order to promote uniform coking throughout the particles and therefore avoid forming peripheral deposits of coke which may impede the diffusion of styrene throughout the catalyst interior.

EXPERIMENTAL

The catalyst used in this study was supplied by Criterion Catalyst Co., identified as C-HDS-1442B, a bimodal resid hydrotreating catalyst used in commercial residual oil demetallation and desulfurization processes. This report discusses data which were gathered in two different studies. Baumgart (*9*) prepared and characterized a series of samples ranging in coke content from 0 to 9.2 wt.%. Following that work two samples with higher coke contents were prepared and studied by Y. Wang.

The coking procedure involved passing a dilute styrene–helium mixture over a thin bed of crushed (−35 to +65 mesh) catalyst at 425°C for a measured period of time. The sample, spread thinly on a Pyrex tray, was purged with helium for one hour (150 ml/min) and then coked with 0.8% styrene in helium for the desired time.

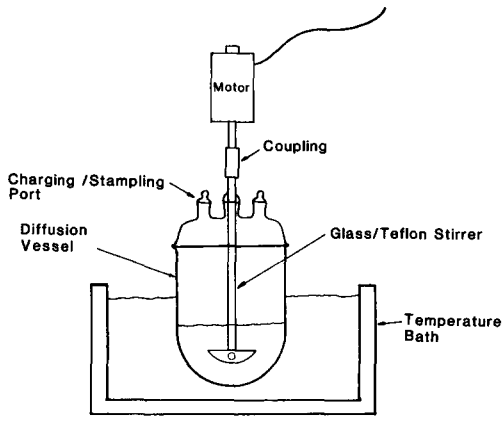

FIG. 1. Schematic of diffusion vessel.

Nitrogen porosimetry analyses were obtained using a Quantachrome Autosorb-6 Automated Nitrogen Porosimeter. Porosity calculations involved a BJH (*10*) analysis using *t*-data of de Boer (*11*) from adsorption and desorption isotherms at 77.4 K. Samples were outgassed in vacuum (0.01 torr) at 120°C for 20 h.

Mercury porosimetry analyses were generated using a Quantachrome Autoscan-60 mercury porosimeter using approximately 1.0 g of catalyst. Samples were outgassed in vacuum (0.01 torr) for 1 h at 95°C. An arbitrary mercury contact angle of 140° and a surface tension of 480 erg cm^2 (dynes/cm) were used to calculate pore size distribution data from the mercury intrusion–extrusion curves.

The diffusion rate of coronene was determined by Baumgart (*9*) for samples ranging in coke content from 0 to 9.2%, using a method described by Chantong and Massoth (*12*) and Johnson *et al.* (*13*). Approximately 0.8 g of coked catalyst were charged with 400 ml of 0.024 g/L coronene in cyclohexane solution in a 500-ml flask (Fig. 1).

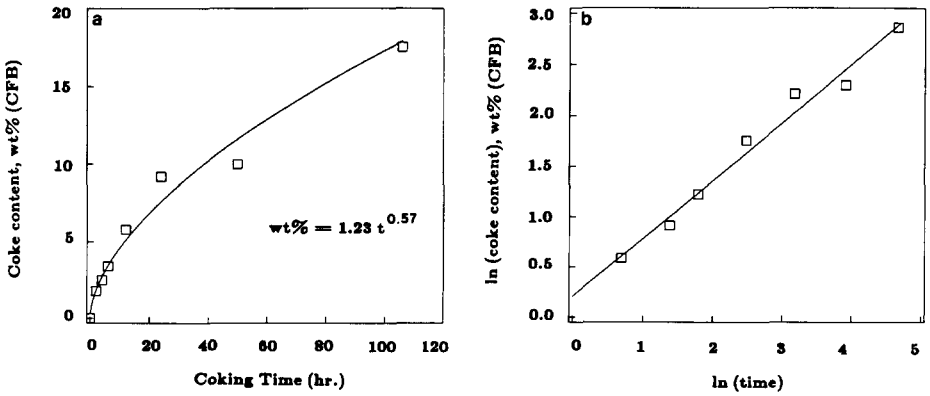

FIG. 2. (a) Change in coke content with time during catalyst treatment (CFB = coke free basis). (b) Logarithmic relationship between coke content and time of catalyst treatment.

Two-ml samples of solution were removed and analyzed after various contact times. UV analyses were conducted with a Beckmann Model 25 UV-spectrophotometer scanning between 330 and 360 nm.

The coke levels on catalyst were determined by a combustion method using a Perkin Elmer Model TGS-2 Thermogravimetric Analyzer with System-4 T. A. Microprocessor. Between 4 and 10 mg of catalyst were used in each determination. The apparatus was purged with helium at 200 cm^3/min and then temperature ramped to 400°C at 15°C/min, followed by a soak at constant temperature for 1 h or until no further weight change could be observed. The gas stream was then switched to hydrogen and the sample reduced for 2.5 h at 400°C, followed by a 1.5-h purge with helium and combustion in air at 500°C for a further 5 h.

RESULTS

Kinetics of Coke Formation

A plot showing the deposition of coke on the catalyst with time is presented in Fig. 2a,b. The same result is found everywhere in the literature of catalyst deactivation and is a correlation of the form

$$C_c = A\theta^n,$$

where C_c is the concentration of coke on catalyst, A and n are the correlation constants, and θ is the length of the processing period (*14*). This relationship was first reported based on empirical evidence by Voorhies (*15*) in 1945. In work reported here, $A = 1.23$ and $n = 0.57$. One interpretation of this correlation and its apparent independence of space velocity (*16*) and low temperature sensitivity is that coking is a diffusion-controlled process (*17*). However, there is much evidence to conclude that coke formation, in general, may or may not be diffusion-controlled, depending upon the catalyst, reactant, reaction conditions, and all other factors which pertain to such rate limitations (*1, 8, 18*).

Nitrogen Adsorption/Desorption Analyses

The influence of coke deposition on pore volume, measured from the nitrogen adsorption isotherm at $P/P_0 = 0.992$, is shown in Fig. 3. The two curves represent pore volumes for coked catalyst and coke-free catalyst respectively. Figure 4 shows that surface area decreases as pore volume decreases in the coked samples.

A careful analysis of the adsorption–desorption isotherms and pore size distributions reveals:

(i) a small drop in pore volume in pores of apparent diameter between 20 and 30 Å

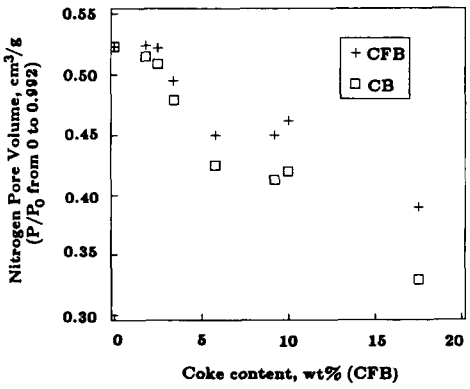

FIG. 3. Change in nitrogen pore volume with coke content.

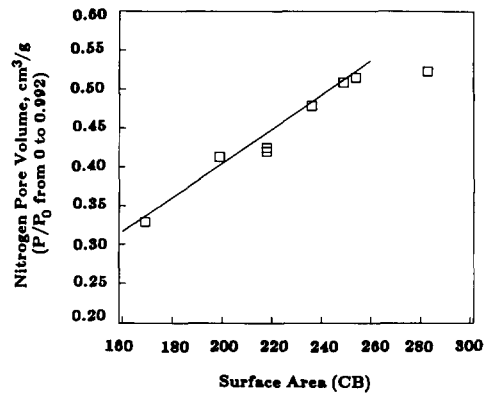

FIG. 4. Change in nitrogen pore volume with surface area.

evident in the adsorption pore size distribution analysis for the fresh catalyst and the coked catalysts (Fig. 5);

(ii) almost identical median pore diameters for the fresh and coked catalysts (Table 1) measured from the desorption pore size distributions;

(iii) the appearance of some pore volume in pores of less than 50 Å diameter for the 10% and 17.5% coke samples, Fig. 6;

(iv) small, but significant, increases in the area of the hysteresis loops when the isotherms are compared on a normalized basis (Fig. 7a,b).

Mercury Pore Size Distributions

Pore size distributions from both mercury intrusion and extrusion for six of the eight samples, plotted with the pore volumes normalized, are shown in Fig. 8. Figure 9 shows

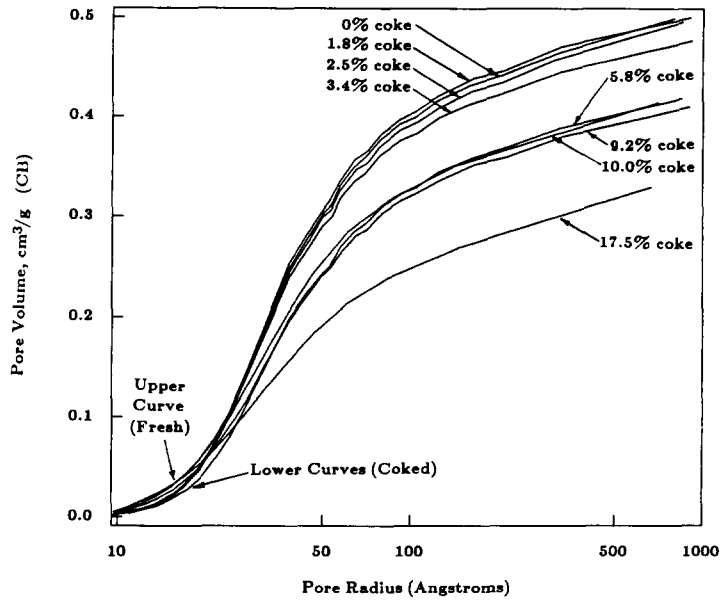

FIG. 5. Integral plots of nitrogen pore size distributions from the adsorption isotherms.

TABLE 1

Nitrogen Adsorption–Desorption and Pore Diffusivity Analysis

Coking time h	Coke content wt.% (CFB)	Surface area (CB) M^2/g	Pore volume (N_2) $P/P_0 = 0.992$ (CB) cm^3/g	Median pore diameter by desorption Å	Isotherm hysteresis area (arb. unit)	Coronene diffusivity $m^2/s \times 10^{10}$
0	0	283	0.523	56	1.93	4.4
2	1.8	254	0.515	54	2.00	4.1
4	2.5	249	0.509	54	1.95	3.8
6	3.4	236	0.479	54	2.16	3.7
12	5.8	218	0.425	54	2.30	3.2
24	9.2	199	0.413	54	2.28	3.7
50	10.0	218	0.420	54	2.22	–
106	17.5	169	0.329	54	2.53	–

the influence of coke level on mercury pore size distributions from the extrusion (9a) and intrusion (9b) curves. Data from all the analyses are reported in Table 2. Several features are significant:

(i) in parallel with the nitrogen data, mercury pore volumes decrease with an increase in coke, and the decrease is associated entirely with a loss in mesoporosity (pore volume in pores of 30–200 Å diameter);

(ii) the intrusion curves show small, stepwise shifts in modal pore diameter from 64 to 51 Å diameter;

(iii) the extrusion curves reveal a major change in shape and position as coke increases on the catalyst;

(iv) mercury retained within the pore structure after complete depressurization decreases gradually as coke increases.

The most dramatic change evident in the porous structure of the coked catalysts then is in the shapes and positions of the mercury extrusion curves. The curves move from a position of 2000–4000 Å diameter for the fresh catalyst down to 100–400 Å for the most heavily coked material.

Diffusivity Experiments

The results of coronene diffusivity into the coked catalysts are reported in Table 1. It would appear that very little decrease in diffusivity occurs as the coke increases on the catalysts from 1.8 to 9.2%. In the light of the nitrogen and mercury porosimetry experiments, reported in Tables 1 and 2, these results are perhaps not surprising. If diffusivity of coronene is limited by the size of the entrance pores, very little change in the sizes of these access pores has occurred during coking. (Access pore sizes are identified as 'Median pore diameter by desorption' in Table 1 and 'Modal pore diameter by mercury intrusion' in Table 2.)

DISCUSSION

The decrease in pore volume as coke increased on the catalyst is not surprising. As reported by others, this does not imply a volume-filling process by coke but rather a pore-blocking action, isolating regions of porosity (*19*). Consequently both surface area and pore volume decrease in a linear, stepwise manner.

Subtraction of nitrogen pore volumes from those measured by mercury intrusion for the samples (coke free basis) reveals a constant value for porosity in macropores (i.e., pores of greater than 500 Å diameter). Similarly, mercury pore volumes measured from the intrusion curves at 500 Å diameter are essentially constant with increasing

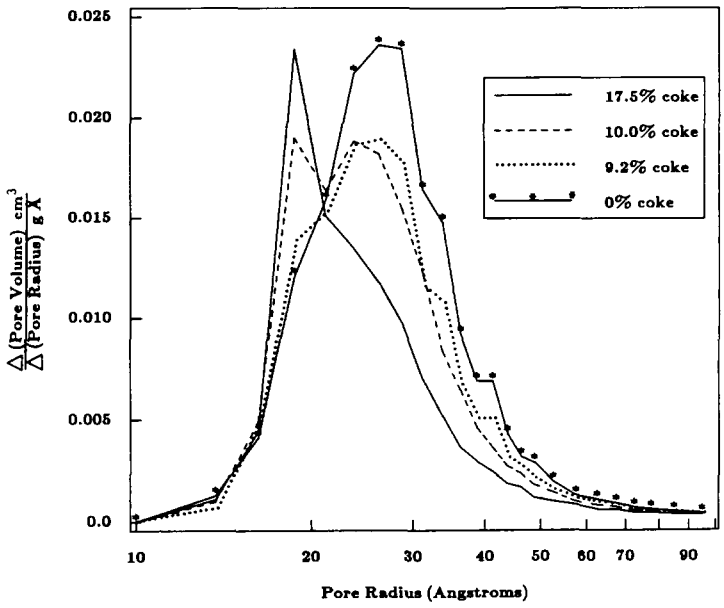

FIG. 6. Influence of coking on nitrogen pore size distributions (desorption).

coke deposition (Table 2). Coke does not, therefore, appear to be depositing in macropores.

If coke deposition occurred uniformly through the catalyst structure pores would be expected to narrow, shifting median pore sizes to smaller values. The fact that this is not occurring further supports the concept of pore blockage. For the 10 and 17.5% coke samples, some pore narrowing is evident,

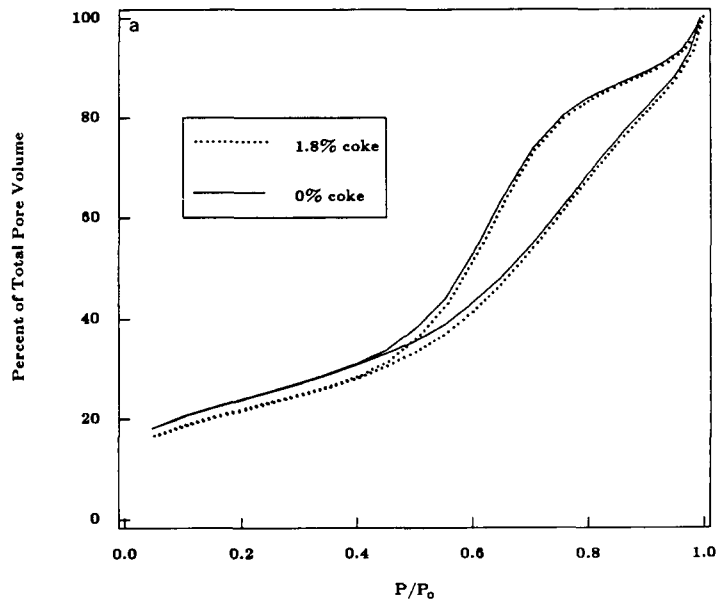

FIG. 7a. Influence of coking on nitrogen adsorption–desorption hysteresis.

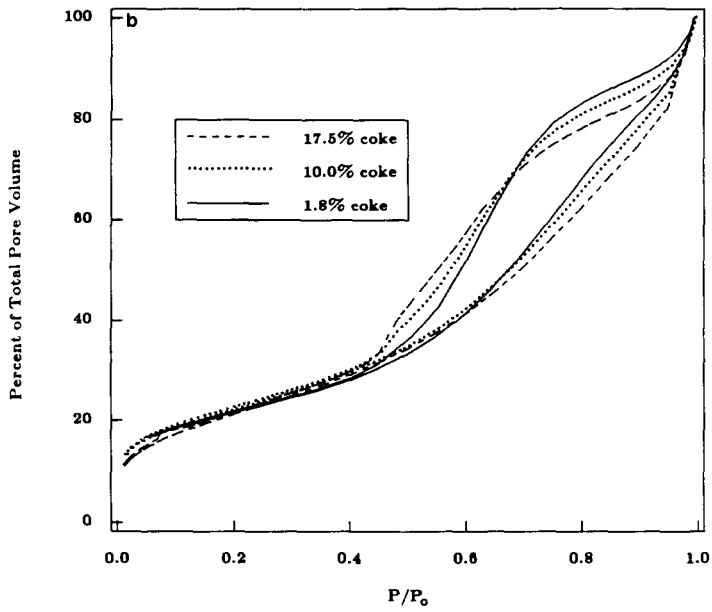

FIG. 7b. Influence of coking on nitrogen adsorption–desorption hysteresis.

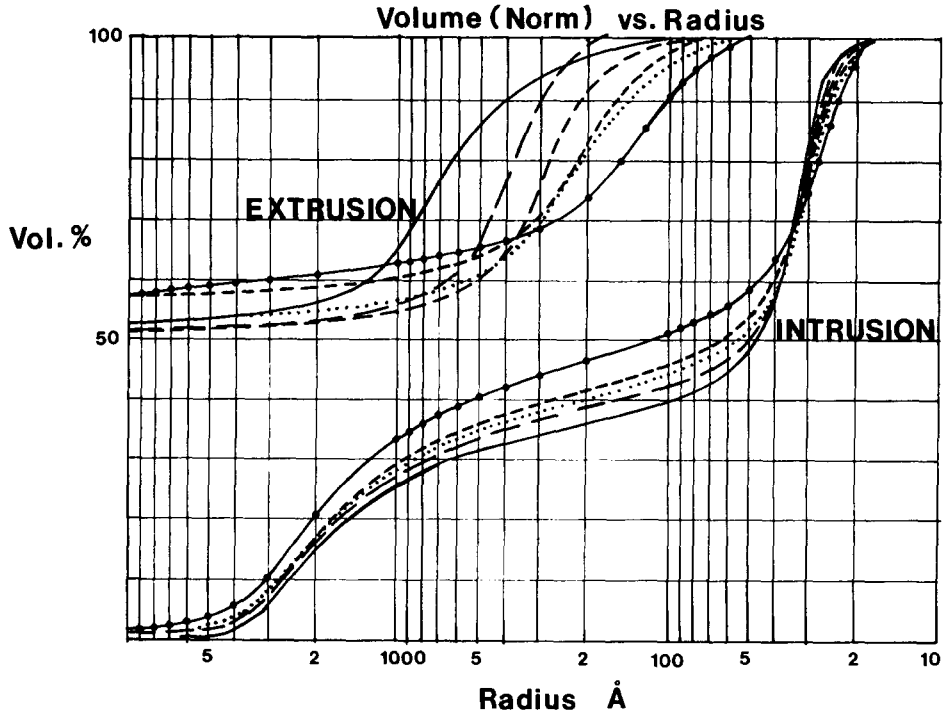

FIG. 8. Mercury intrusion and extrusion porosimetry curves normalized to 100 volume% (coked basis) for (———) fresh catalyst; (——) 1.0% coke; (———) 3.4% coke; (----) 9.2% coke; (· · · · ·) 10.0% coke; (-●-●-●-) 17.5% coke.

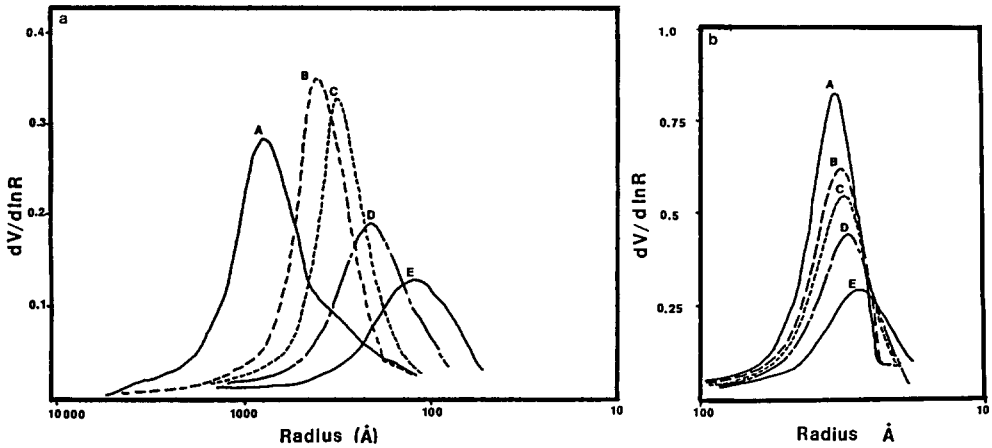

FIG. 9. Mercury pore size distributions (differential plots) for fresh and coked catalysts from (a) the extrusion and (b) the intrusion curves for (A) fresh catalyst; (B) 1.8% coked catalyst; (C) 3.4% coked catalyst; (D) 9.2% coked catalyst; (E) 17.5% coked catalyst.

particularly for the latter sample, and a small peak appears in the nitrogen desorption differential plot (Fig. 6) near 36 Å diameter.

A drop in pore volume measured from the nitrogen adsorption isotherm in pores of between 20 and 30 Å diameter implies a loss of wedge-shaped pores which are believed to fill and empty of nitrogen reversibly. This loss occurs for even the least coked sample. Such pores are probably not involved in pore blockage. They are more likely associated with the interparticulate spaces close to the points of contact between particles.

Changes in the position of the mercury extrusion curve (i.e., shifts toward apparently smaller pores with increasing coke) are not reflected in the nitrogen desorption pore size changes. The nitrogen data seem to support a pore size of 55 Å regardless of coke level. The changes (ca. 60 down to 51 Å diameter) reported by mercury intrusion are probably due to small changes in mercury contact angle as coke levels increase.

The pore size distributions for the coked catalysts, calculated from the nitrogen desorption isotherms, are similar to those determined from the mercury intrusion curves, when limited to the mesopore region (30–200 Å). This is the pore size region which would be expected to have the greatest effect on coronene diffusivity. Since very little change in pore size occurs during coking, it is no surprise that coronene diffusivity does not change significantly.

These results imply that no change, or very little change has occurred in the ability of large molecules to gain access into the catalyst particle even after considerable coke deposition. This contrasts sharply with the results of Johnson *et al.* (*13*) who studied coronene diffusivity in fresh and aged residual oil demetallation catalysts. In their work they reported low diffusivities for coronene in aged catalysts but concluded that low diffusivities were due to metal deposition at the pore mouths on the outer edge of the particles rather than to coke plugging. Also, the diffusivities of coronene in the aged catalysts were found to increase as the access pore size of the original catalyst increased. Hence, taking both studies, coking alone appears not to lower the diffusivity of large reacting molecules but rather lowers the overall surface area and pore volume available for reaction.

On the other hand, changes in the mercury extrusion curves during depressurization are quite dramatic. The reason for this is not obvious, primarily because the theory of mercury extrusion porosimetry is still in

TABLE 2

Mercury Porosimetry Analysis[a]

Coking time h	Coke content, wt.%	PV(Hg) 60k (CB) cm^3/g	PV(Hg) 50k–10k (CB) cm^3/g	PV(Hg) 4.18k (CB) cm^3/g	Modal pore diameter by intrusion Å	PV(Hg) entrapped (CB) cm^3/g	PV(Hg) 60k (CFB) cm^3/g	PV(Hg) 50k–10k (CFB) cm^3/g	PV(Hg) 4.18k (CFB) cm^3/g	PV(Hg) entrapped (CFB) cm^3/g
0	0	0.787	0.465	0.277	64	0.407	0.787	0.465	0.277	0.407
2	1.8	0.668	0.379	0.249	60	0.336	0.680	0.386	0.254	0.342
4	2.5	0.671	0.375	0.249	60	0.335	0.688	0.385	0.255	0.344
6	3.4	0.631	0.346	0.243	60	0.325	0.653	0.358	0.252	0.336
12	5.8	0.586	0.322	0.234	60	0.313	0.622	0.342	0.248	0.332
24	9.2	0.569	0.294	0.230	56	0.318	0.627	0.324	0.253	0.350
50	10.0	0.576	0.302	0.225	55	0.293	0.640	0.336	0.250	0.326
106	17.5	0.481	0.214	0.216	51	0.254	0.583	0.259	0.262	0.308

[a] Surface tension = 474 erg/cm^2; contact angle = 140°; PV = cumulative volume to designated pressure in psig.

its infancy. One explanation might suggest that a change has occurred in the retreating mercury contact angle as the coke level increased (*20, 21*). The mercury contact angle is a parameter which is needed to convert measured pressures from the porosimetry experiment into pore radii, using the Washburn equation (*22*). Throughout this report a single value for the mercury contact angle of 140° has been used, although it is well understood that use of another value would generate small differences in absolute values of the pore size. Opting for a single value is not without merit since the correct value is almost impossible to predict for every sample. Assuming that this is an acceptable approach it is most unlikely that such large changes in the extrusion pore radii reported here could have been due to changes in contact angle on the coked surfaces. In support of this is the evidence that only small shifts in the intrusion curves have been recorded as coking increased.

The hysteresis common to mercury porosimetry, intrusion–extrusion experiments, cannot be explained in terms of a parallel bundle of nonintersecting pores without resort to these contact angle change arguments. However, modeling studies (*23–27*) have, more recently, assisted in providing an alternative explanation which invokes the concept of a porous network. This is sometimes referred to as a stochastic network of pores where pores of different sizes are connected in a 3-dimensional structure via other pores. The extrusion (or retraction) curve is then an indication of the pore size of the draining pore (using the Washburn equation (*22*) and the extent of the network. Large diameter pores which are only accessed via smaller pores are referred to as "shielded" (*28*) or "shadowed" (*23*) pores. Weist *et al.* (*27*) make use of this type of model in a study of the change in morphology of polymerization catalysts as polyethylene forms in the catalyst pore structure. In that study there was a shift in pore distribution (pore bodies) to smaller sizes with increase in polymerization.

A much more plausible explanation of the current data can then be derived, supporting the nitrogen data shown above. Increased coke deposition causes pore blockage, first in narrow, connecting pores within the structure. The mechanism is probably similar to that described by El-Kady and Mann (*29*) where wedge layering of coke deposits in connecting pores results in reduced access of mercury through these narrow pores into the large, shielded pores beyond. Since mercury can no longer fill these shielded pores, penetration progresses only to the coke seals within the connecting pores.

This explanation suggests that coking occurs first within the network structure at intersections between the largest diameter shielded pores and the small diameter connecting pores. Once these large pores are sealed off, the next smaller range of pore sizes of shielded pores experience coking at intersections with small connecting pores (Fig. 10), until they too become sealed off. In Fig. 9 curves of differential pore size distribution are shown for the pores which have survived following coking. The curves represent a picture of the pores which are shielded in the fresh catalyst.

During depressurization, mercury will then retract more easily (i.e., at higher pressures, corresponding to shielded pore sizes which are smaller than previous). This retraction now occurs via open connecting pores to the particle exterior surface. As each range of shielded pore becomes sealed off from access from the particle exterior, the mercury retracts sooner, at smaller and smaller apparent pore sizes. At the ultimate condition of 99%-plus coked catalyst, one might imagine the mercury intrusion from the exterior surface through access pores will retract following the same pressure/volume curve as the intrusion.

Why are these features not apparent in the hysteresis loops of the nitrogen isotherms? Probably because adsorption of nitrogen in the large, "shielded" pores is occurring at pressures so close to saturation that the resolution of the pore size analysis technique

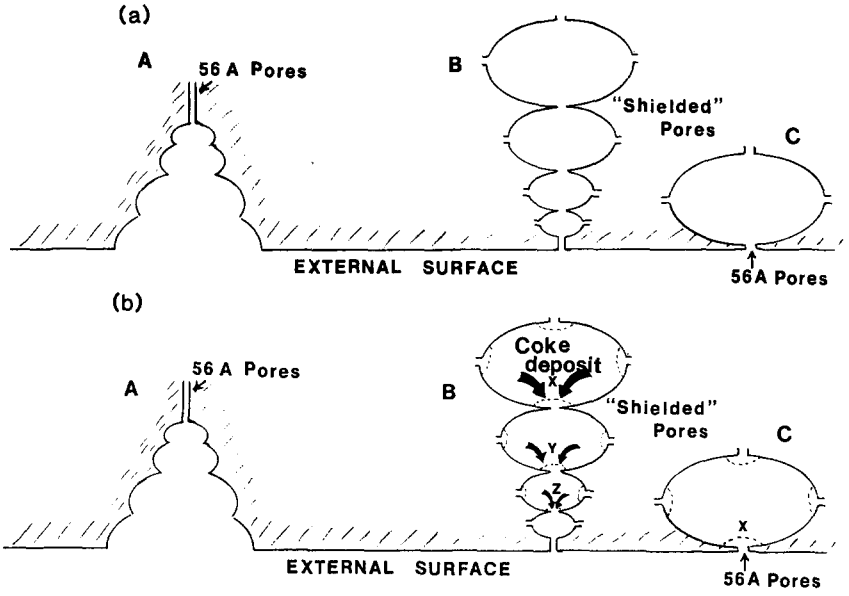

FIG. 10. Schematic representation of a part of the porous network of the fresh (a) and coked (b) catalyst. Mercury intrusion curve reflects intrusion into "A" pore network as filling of macropores but into "B" and "C" pore networks as intrusion into mesopores. Following an initial light coking, it is proposed that coke plugging occurs first at connections between the largest "shielded" pore and the small pore (at X). Mercury intrusion shows a loss of mesopore volume due to a loss of 56 Å pores. Following further stages of coking, plugging occurs sequentially at "Y" and "Z."

is not adequate. On emptying, desorption occurs from the small connecting pore "throats," the size of which change very little on coking.

Sharatt and Mann (*28*) discussed the implications of the network model for diffusion and reaction. In their study three model networks were proposed, 10 × 10, 20 × 20 and 30 × 30, with either single-sized pores, uniform pore size distribution (20–2000 Å), or bimodal pore distributions (80% pore volume in pores of 60 Å diameter and 20% in pores of 2000 Å diameter), and were compared with the equivalent parallel bundle models. The effects of changing the pore size distribution and the Thiele modulus on the catalyst effectiveness were then investigated. A first-order, irreversible kinetics reaction was chosen.

The greatest changes in effectiveness factor were predicted for the bimodal distributions networks when compared to the parallel bundle model. For high Thiele modulus conditions the predictions for network and parallel bundle distribution functions are similar; however, at low and medium Thiele modulus, the effect of shielding of the large pores predominates. Put another way, pore structure 'tortuosities' vary with Thiele modulus for bimodal pore size distribution catalysts than for uniform or single pore size distribution catalysts when viewed in terms of stochastic pore networks. Such differences would account for catalyst selectivity differences for reactions which are diffusion controlled.

CONCLUSIONS

The effect of coke deposition on the porosity of a bimodal residual oil hydrotreating catalyst has been investigated. Evidence is presented for the role of the porous network in the catalyst. The importance of pores which are shielded within the structure has been identified. Large shielded pores appear to seal off first during coking, followed by

the next smaller size range of shielded pores. It is proposed that coking occurs first at the junctions between the large shielded pores and the narrow connecting pores.

REFERENCES

1. Tamm, P. W., Harnsberger, H. F., and Bridge, A. G., *Ind. Eng. Chem., Process Des. Dev.* **20,** 262 (1981).
2. Dautzenberg, F. M., van Klinken, J., Pronk, K. M. A., Sie, S. T., and Wiffels, J.-B., *in* 5th International Symposium on Chemical Reaction Engineering, Houston, 1978," p. 254.
3. Nielson, E., *Ind. Eng. Chem., Process Des. Dev.* **14,** 27 (1975).
4. Hannerup, P. N., and Jacobsen, A. C., *Prepr. Amer. Chem. Soc. Div. Pet. Chem.* **28,** 576 (1983).
5. Bridge, A. G., *in* "Advances in Catalytic Chemistry, II, Salt Lake City, 1982."
6. Prasher, B. D., Gabriel, G. A., and Ma, Y. H., *Ind. Eng. Chem., Process Des. Dev.* **17,** 266 (1978).
7. Gutberlet, L. C., and Bertolacini, R. J., *Ind. Eng. Chem., Prod. Res. Dev.* **22,** 246 (1983).
8. Levinter, M. E., Panchenkov, G. M., and Tanatarov, M. A., *Int. Chem. Eng.* **7,** 23 (1967).
9. Baumgart, Jerry, "Characterization of a CoMo/Al_2O_3 Catalyst Exposed to a Coke Inducing Environment," M. S. Thesis, Georgia Institute of Technology, Atlanta, GA 30332.
10. Barrett, E. P., Joyner, L. G., and Halenda, P. H., *J. Amer. Chem Soc.* **73,** 373 (1951).
11. de Boer, J. H., "The Structure and Properties of Porous Materials," p. 68, Butterworths, London, 1958.
12. Chantong, A., and Massoth, F. E., *AIChE J.* **29,** 725 (1983).
13. Johnson, B. G., Massoth, F. E., and Bartholdy, J., *AIChE J.* **32,** 1980 (1986).
14. Butt, J. B., "Catalyst Deactivation," AIChE Today Series, AIChE, pp. 1–23, 1974.
15. Voorhies, A., *Ind. Eng. Chem.* **37,** 318 (1945).
16. Eberly, P. E., Kimberlin, C. N., Miller, W. H., and Drushel, H. V., *Ind. Eng. Chem., Proc. Des. Dev.* **5,** 193 (1966).
17. Ozawa, Y., and Bischoff, K. B., *Ind. Eng. Chem. Proc. Dev.* **7,** 67 (1968); Ozawa, Y., and Bischoff, K. B., *Ind. Eng. Chem. Proc. Dev.* **7,** 72 (1968).
18. Butt, J. B., Delgado-Diaz, S., and Muno, W. E., *J. Catal.* **37,** 158 (1975).
19. Beekman, J. W., Froment, G. F., and Pismen, L., *Chem. Ing. Tech.* **50,** 960 (1978); Beekman, J. W., and Froment, G. F., *Ind. Eng. Chem. Fundam.* **18,** 245, (1979).
20. Lowell, S., and Shields, J. E., *J. Colloid Interface Sci.* **80,** 192 (1981).
21. Lowell, S., and Shields, J. E., "Powder Surface Area and Porosity," 2nd ed., p. 126, Chapman & Hall, London, 1984.
22. Washburn, E. W., *Proc. Natl. Acad. Sci. U.S.A.* **7,** 115 (1921).
23. Conner, W. C., Lane, A. M., Ng, K. M., and Goldblatt, M., *J. Catal.* **83,** 336 (1983).
24. Androutsopoulos, G. P., and Mann, R., *Chem. Eng. Sci.* **34,** 1203 (1979).
25. Shah, N., and Ottino, J. M., *Chem. Eng. Sci.* **42,** 73 (1987).
26. Ferrillo, R. G., and Carruthers, J. D., "Crystallinity of Pseudoboehmite in Precipitated Alumina: Thermal Analysis Studies," 17th North American Thermal Analysis Society Conference, Orlando, FL, October 1988.
27. Weist, E. L., Ali, A. H., Naik, B. G., and Conner, W. C., *Macromolecules* **22,** 3244 (1989).
28. Sharratt, P. N., and Mann, R., *Chem. Eng. Sci.* **42,** 1565 (1987); Mann, R., and Sharratt, P. N., *Chem. Eng. Sci.* **43,** 1875 (1988).
29. El-Kady, F. Y. A., and Mann, R., *Appl. Catal.* **3,** 211; (1982); El-Kady, F. Y. A., and Mann, R., *J. Catal.* **69,** 147 (1981).